Available online at www.sciencedirect.com
ScienceDirect
Acta Materialia 55 (2007) 1343–1349
Acta MATERIALIA
www.actamat-journals.com

# Scaling equation for yield strength of nanoporous open-cell foams

A.M. Hodge [a,*], J. Biener [a], J.R. Hayes [a], P.M. Bythrow [a], C.A. Volkert [b], A.V. Hamza [a]

[a] Nanoscale Synthesis and Characterization Laboratory, Lawrence Livermore National Laboratory, P.O. Box 808, L-352, Livermore, CA 94550, USA
[b] Institut für Materialforschung II, Forschungszentrum, Karlsruhe, Germany

Received 8 June 2006; received in revised form 27 September 2006; accepted 28 September 2006
Available online 22 December 2006

**Abstract**

A comprehensive study on the relationship between yield strength, relative density and ligament sizes is presented for nanoporous Au foams. Depth-sensing nanoindentation tests were performed on nanoporous foams ranging from 20% to 42% relative density with ligament sizes ranging from 10 to 900 nm. The Gibson and Ashby yield strength equation for open-cell macrocellular foams is modified in order to incorporate ligament size effects. This study demonstrates that, at the nanoscale, foam strength is governed by ligament size, in addition to relative density. Furthermore, we present the ligament length scale as a new parameter to tailor foam properties and achieve high strength at low densities.


*Keywords:* Nanoporous; Foams; Nanoindentation; Dealloying

## 1. Introduction

The effects of scaling (macro to nano) on the mechanical behavior of materials has been a subject of intensive studies and discussion [1–6]. As new materials such as nanoporous foams are developed, scaling relationships are constantly redefined. In bulk materials it has been shown that, at the nanoscale (<100 nm), grain size and sample size affect the overall mechanical behavior and give rise to very distinct mechanical properties, such as higher strength [4,6,7]. Therefore, it is expected that nanoporous materials with pores sizes <100 nm would also behave differently from macrocellular foams.

Gibson and Ashby [8] have developed scaling equations for open-cell and closed-cell foam by using mathematical relationships between the foam relative density (ratio of the density of the foam to the density of the bulk material) and the bulk material mechanical properties. Their equations are derived using the mechanics of deformation on an ''idealized'' cell geometry in conjunction with mechanical test data from macro pore size foams. These scaling equations have been shown to describe quite well the overall foam behavior for many different types of macrocellular (micron and millimeter size pores) foams [9–13].

In the case of nanoporous foams, there has been no previous research providing a systematic study of the scaling equations and how they correspond at the nanoscale. Dealloyed gold foams provide an excellent system for such a study, since they can be synthesized with a wide range of densities as well as a wide range of pore sizes (nanometers to microns) without changing the overall morphology [14]. In the case of nanoporous gold foam, there are at least three available methods to change the ligament size: (a) the dealloying method (free corrosion vs. potentiostatically driven); (b) the variation of total dealloying time [15]; and (c) post-dealloying furnace annealing [16].

There have been a number of studies on the mechanical behavior of nanoporous materials and values have been reported for yield strength and elastic modulus. For example, Li and Sieradzki [16] reported a ductile–brittle transition in porous Au, which seemed to be controlled by the microstructural length scale of the material. Biener et al. reported on the high yield strength of nanoporous Au

* Corresponding author. Tel.: +1 925 424 3715; fax: +1 925 423 7496.
*E-mail address:* hodge4@llnl.gov (A.M. Hodge).

1359-6454/$30.00 
doi:10.1016/j.actamat.2006.09.038

foams [17] and their fracture behavior as a function of the length scale [18]. More recently, Volkert et al. have performed micro-compression tests on dealloyed nanoporous Au foam columns (36% relative density, 5–10 at.% residual silver) and have suggested that the Gibson and Ashby equation should be modified by substituting the yield strength of fully dense Au (2–200 MPa) to account for the increase in measured yield stress [19]. Additionally, Biener et al. presented a similar conclusion about the need to account for the scaling effects which relate strength and ligament size [20].

In this paper, we present a comprehensive study of open-cell nanoporous Au foams with relative densities ranging from 20% to 42% and compare the experimental values to the Gibson and Ashby scaling equation for yield strength. We address issues such as ligament size, pore size and relative density in order to present a link between the mechanical behavior in nanoporous foams to macropore-size foams. A modified scaling formula is presented relating relative density and ligament size to the foam yield strength.

## 2. Experimental

### 2.1. Foam processing

The nanoporous Au samples used in the present study were made by electrochemically driven dealloying or free corrosion of Au/Ag alloys. Polycrystalline $Au_xAg_{100-x}$ (where $x = 42$–$20$ at.%) alloy ingots were prepared from an Au (99.999%) and Ag (99.999%) melt at 1100 °C and homogenized for 100 h at 875 °C under argon. Disks approximately 5.0 mm in diameter and 300 μm thick were cut from the alloy ingots, polished on one side, and then heat-treated for 8 h at 800 °C to relieve stress. The alloy composition was confirmed by a fire assay technique.

Nanoporous Au samples prepared by selective electrolytic dissolution were dealloyed in 1 M $HNO_3$ and 0.01 M $AgNO_3$ solution. A three-electrode electrochemical cell controlled by a potentiostat (Gamry PCI4/300) was used for these experiments. Dealloying was performed at room temperature, using a platinum wire counter electrode and a silver wire pseudo-reference electrode. The alloy samples were held at an applied electrochemical potential between 600 and 900 mV for a period of 2–3 days until the dissolution current measurement was negligible. The nanoporous samples prepared by free corrosion were submerged in a 67–70% $HNO_3$ solution for 2–3 days until no further weight loss was detected.

In order to produce a sample with multiple pore/ligament sizes, a 30% relative density sample was divided into five slices, and each slice was subsequently subjected to heat treatment in air for 2 h at 200, 300, 400 and 600 °C.

### 2.2. Foams characterization and testing

Scanning electron microscopy (SEM), transmission electron microscopy (TEM) and X-ray diffraction (XRD) were employed for microstructural characterization. TEM samples were prepared by microtome slicing as well as focused ion beam (FIB) milling. Energy-dispersive X-ray (EDX) spectra were collected for all nanoporous Au samples, thus confirming that the remaining Ag concentration was less than 1.0 at.% after dealloying. The sample density was then estimated using the starting alloy composition, and the remaining Ag content was estimated by assuming no volume shrinkage. The thickness and diameter of the sample were measured before and after dealloying; dimensional changes were determined to be negligible. Additionally, the calculated sample volume and measured mass (before and after dealloying) were utilized to verify sample density.

The mechanical properties of nanoporous Au were tested by depth-sensing nanoindentation using a Triboindenter (Hysitron) with a Berkovich tip (radius of ~200 nm). Indentations were performed on the planar, "polished surface" (polished before dealloying) of the sample disks as well as on cross-sections produced by fracturing the sample. All foam nanoindentation experiments were performed using a constant loading rate of 500 μN/s, with loads ranging from 200 to 4000 μN. A minimum of 125 indents, performed in groups of 25 were collected for each sample.

## 3. Results

### 3.1. Dealloying results

As mentioned in Section 1, the use of different dealloying techniques allows us to alter the ligament scales of the foams. Since Au does not oxidize in air even at elevated temperatures, the pore/ligament dimensions can easily be fine-tuned between ~100 nm and 1 μm by a simple furnace anneal. The underlying principle behind all these methods is Ostwald ripening, by the formation of more thermodynamically stable larger structures by diffusion. However, in order to make a complete assessment of the mechanical properties, a wide range of densities is also necessary. Currently, Au foam can be produced by dealloying, in a range between 20% and 40% relative density. Relative densities below 20% and above 60% are limited by percolation limits when using Ag/Au alloy [21,22]. Furthermore, foams above 40% relative density are expected to have significantly different behavior from lower density foams [8] and therefore will not be discussed in this paper.

Table 1 presents a summary of the results from samples ranging from 20% to 40% relative density given different processing conditions and their corresponding ligament size. The relative density is defined as $\rho^*/\rho_s$, where $\rho^*$ is the foam density and $\rho_s$ is the bulk material density [8]. Fig. 1 shows a 30% relative density Au sample which was divided into five samples, C–G. Sample C was not annealed; sample F was annealed for 2 h at 400 °C and sample G was annealed for 2 h at 600 °C. Samples F and G exhibit pore and ligament size growth up to 15 times larger than the original dealloyed structure.

Table 1
Sample processing method and ligament size

| Relative density (%) | Processing method[a] | Average ligament size (nm) |
|---|---|---|
| 42 A | EC | 100 |
| 42 B | EC | 40 |
| 35 A | FC | 50 |
| 30 A | FC | 50 |
| 30 B | FC | 40 |
| 30 C | FC | 60 |
| 30 D | FC then HT 200 °C, 2 h | 60 |
| 30 E | FC then HT 300 °C | 160 |
| 30 F | FC then HT 400 °C | 480 |
| 30 G | FC then HT 600 °C | 900 |
| 25 A | FC | 50 |
| 25 B | FC | 30 |
| 25 C | EC | 5 |
| 25 D | FC then HT 400 °C | 200 |
| 20 A | EC | 20 |

[a] FC denotes by free corrosion, EC denotes potentiostatically driven and HT denotes heat treatment.

SEM micrographs, similar to those presented in Fig. 1, were used to measure hundreds of pores and ligaments in each sample. Fig. 2 presents the ligament size distribution for 25% and 30% relative density foams. It should be noted that for all unannealed samples, we found the pore-to-ligament size ratio to be ~1. Further details of pore changes as a function of temperature can be found elsewhere [14,16].

### 3.2. Nanoindentation

In the case of plastic indentation, it has been demonstrated that, for foams with relative densities less than 30%, the hardness ($H$) is approximately equal to the yield strength ($\sigma_y$) rather than $H \sim 3\sigma_y$ which characterizes a fully dense material [8]. Therefore, throughout this paper, we will use this assumption to assess the yield strength from the hardness data. A more detailed discussion of the validity of this assumption can be found in Section 4.2.

Fig. 3 shows the loading–unloading curves for the 30% relative density sample as dealloyed and heat treated at 300 and 400 °C with ligament sizes of 60, 160 and 480 nm respectively. One can calculate the hardness and modulus values by analyzing these data using the Oliver–Pharr method [23]. Note that the curves for a given sample overlap independent of indentation depth, thus showing homogeneity through the sample thickness. Fig. 4 represents data for 25% and 30% relative density samples plotted as a function of contact pressure vs. indentation depth. Values from Fig. 4 show that the hardness decreases with increasing indentation depth, and approaches a "steady-state" value for indentation depths greater than 500 nm. Furthermore, hardness values were validated by using the peak indentation load $P_{max}$ to the projected indentation area $A_p$ of the residual indent impression on SEM micrographs [17].

A summary of all tests performed and the Gibson and Ashby prediction for yield strength, Eq. (1), is shown in Fig. 5. Since material values for bulk gold yield stress are quite scattered (10–200 MPa) [24,25], we use the highest value as the input for $\sigma_s$ in Eq. (1). Fig. 5 is a plot of the normalized yield stress vs. relative density, including experimental data and noting data according to the ligament size. It should be emphasized that as the ligament size approaches 1.0 μm the data begin to approach the Gibson and Ashby scaling prediction

$$\sigma^* = C_2\sigma_s\left(\frac{\rho^*}{\rho_s}\right)^{3/2} \quad (1)$$

where * denotes foam properties and $s$ denotes solid properties. The coefficient $C_2$ is 0.3 as given by Gibson and Ashby.

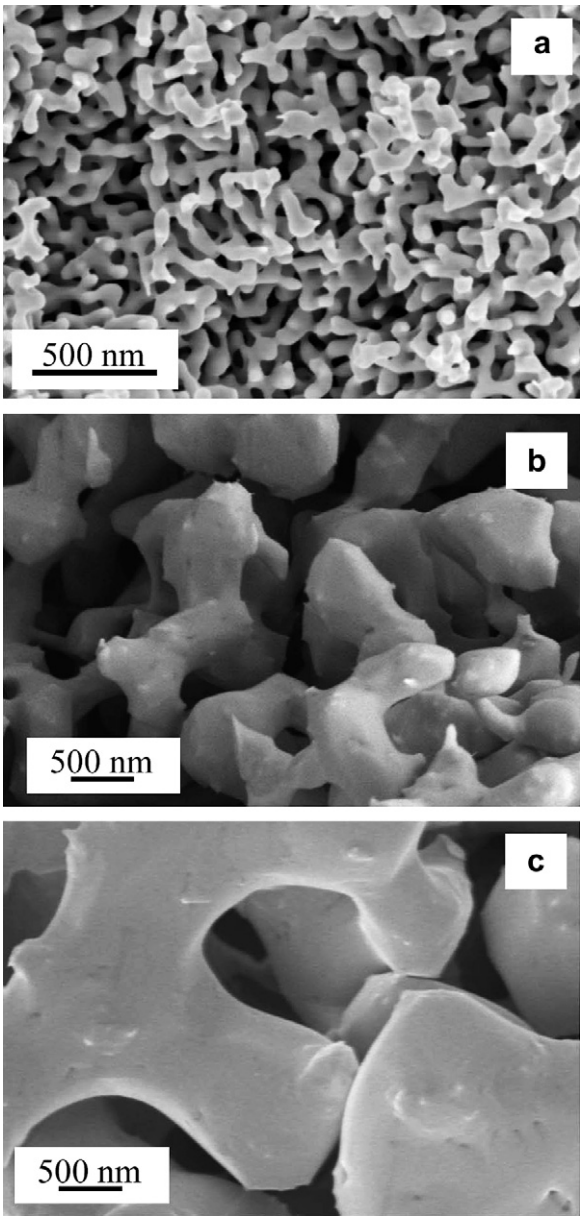


Fig. 1. SEM micrographs of a 30% relative density foam: (a) as prepared by free corrosion (sample C) and then heat treated in air at (b) 400 °C (sample F) and (c) 600 °C (sample G).

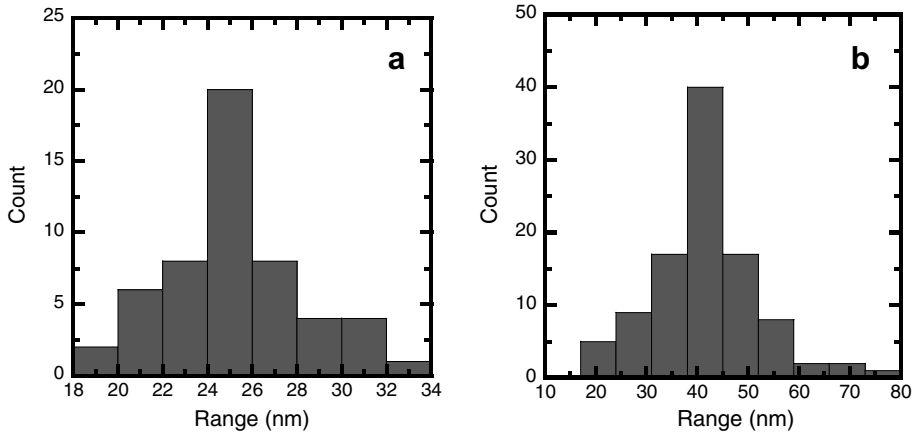


Fig. 2. Distribution of ligament size for two different relative densities: (a) 25%, (b) 30%.

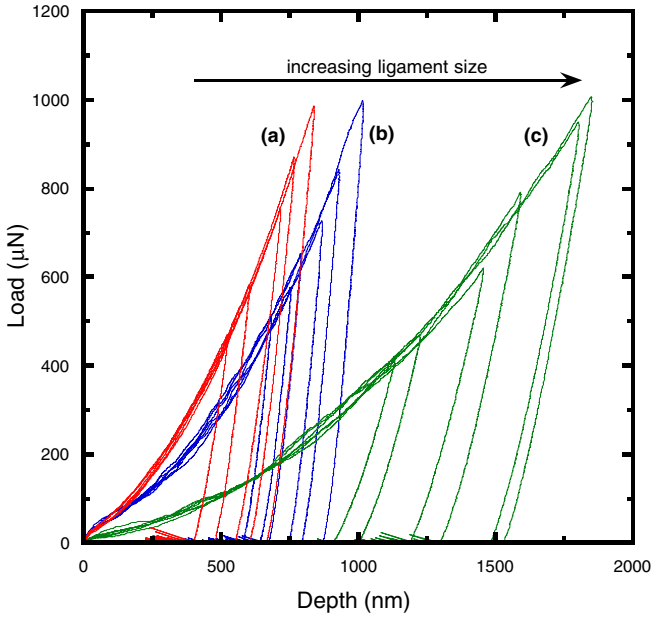


Fig. 3. Nanoindentation loading/unloading curves for 30% relative density sample as a function of ligament size. (a) Sample as prepared by free corrosion; and samples heat treated in air at: (b) 300 °C and (c) 400 °C, given the same load and loading rates (500 μm/s), with ligament sizes of 60, 160 and 480 nm, respectively.

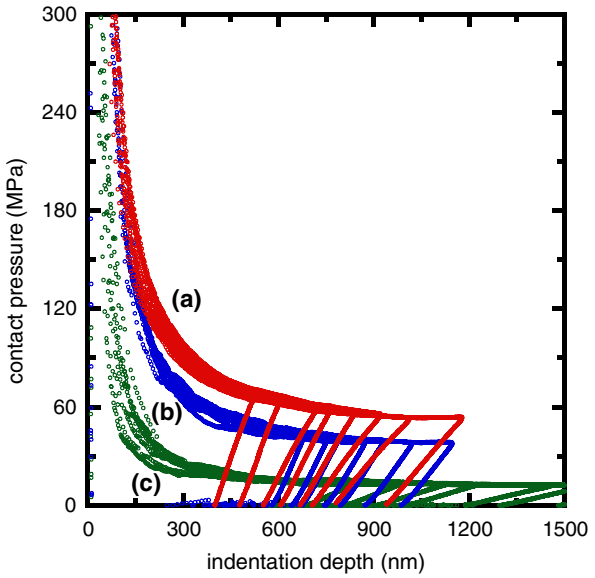


Fig. 4. Nanoindentation data for 30% relative density sample foams plotted as a function of contact pressure vs. indentation depth, given three distinct ligament sizes: (a) 60 nm; (b) 160 nm; and (c) 480 nm.

## 4. Discussion

### 4.1. Nanoindentation technique validation

The use of indentation as a tool to measure foam hardness on macro-size foams is well documented in the literature [26–30]. Strength values from compression and indentation tests have been shown to give equivalent values for low-density foams when the indenter is large relative to the cell size (>10 times the cell size) [26]. Most recently, Chen et al. presented a study comparing nanoindentation, bulge test measurements and finite element analysis as techniques to measure the mechanical properties of thin polymers films (23% porosity) and found that nanoindentation presented similar values to other tests and simulations as long as sample densification was accounted for [31]. In the current study, we use nanoindentation to quantify the nanofoam mechanical behavior. First, we address indentation size effects issues in order to present representative values for each foam. All samples were indented to depths ranging from 100 nm to 2 μm; note that even the deepest indents correspond to less than 1% of the total sample thickness (250–300 μm). In the case of densification effects, it has been shown that, during indentation, the area underneath the indenter is compressed and densified, while the area outside the indentation diameter remains undeformed [26,28,32]. This result is consistent with our previous observations on nanoporous foams [17]. As shown in Fig. 4, we see an exponential decay in hardness as a function of indentation depth, which appears to plateau after indentation depths

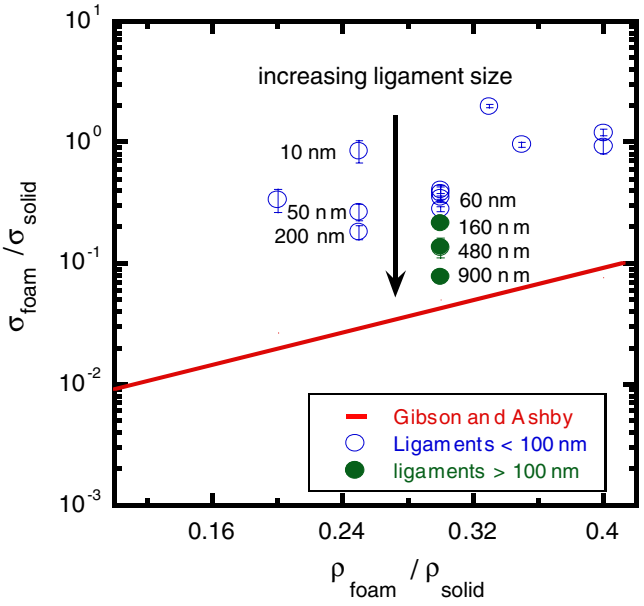


Fig. 5. Experimental values for foam yield stress for all samples shown in Table 1, normalized by the yield stress for fully dense Au. The solid line presents the Gibson and Ashby prediction for a gold foam.

larger than 500 nm. All values presented in Fig. 5 have been taken from this "plateau" area. The issue of indentation size effects was previously addressed by Andrews et al., who performed a detailed study of specimen size effects compared with cell size using indentation on Al open cell (20 pores per in.) foams [26]. Their results show an exponential decay in hardness as a function of the normalized indenter size/cell size [26]. In the current study, a similar effect is observed and appears more pronounced for the samples with smaller ligament size.

Another issue regarding indentation is the assumption that $H \sim \sigma_y$, which characterizes a fully compressible material. During indentation, low-density foam deformation underneath the indenter has been shown to be mostly plastic, and thus mostly compressible; areas outside the indentation area have been shown to remain undeformed, which is consistent with a fully compressible material [17,26,28,32,33]. Although low-density foams have been shown to have non-zero Poisson's ratio [11,19], in the case of indentation we are specifically referring to the "lateral expansion coefficient" or "plastic Poisson's ratio ($\upsilon_p$)", which typically approaches zero for low-density foams [34,35]. For example, the Poisson's ratio of low-density open-cell aluminum (Duocel) foams have been shown to be ~0.25 [11], while the plastic Poisson's ratio is reported to be ~0.052 [34]. Therefore, using the relationship $H \sim \sigma_y$ appears to be a reasonable assumption for low-density nanoporous foams tested by nanoindentation.

### 4.2. Comparison to Gibson and Ashby equations

Due to the possible applications of nanoporous foams, such as for sensors and actuators [36,37], it is important to study the mechanical behavior of nanoporous foams and compare that behavior with their macrocellular counterparts. As shown in Fig. 5, the experimental data for the normalized yield strength vs. relative density of nanoporous foams deviates from the Gibson and Ashby predictions. It has been stated before that this type of nanoporous material is up to 15 times stronger than predicted and approaches the theoretical strength of Au [17].

Previous studies on macrocellular foams have investigated the effects of cell geometry and the relative density of foams, and have concluded that, given a similar porosity, the cell size had a minimal effect in the mechanical behavior [38,39]. However, this is not the case for the nanoporous foams. For example, the 30% relative density samples (A–G in Table 1) have the same relative density and ligament sizes ranging from 40 to 900 nm; in Fig. 5 and Table 1, a strong relationship is observed as a function of ligament size, i.e increasing the ligament size decreases the hardness or yield strength. The same effect can be seen for the 25% relative density sample for three distinct ligament sizes (created by changing dealloying conditions): 10, 30 and 50 nm. It should be noted that, as the ligament size approaches 1.0 μm (sample 30 G), the data begin to approach the Gibson and Ashby prediction. Note that the hardness/yield strength standard deviation for all samples in Fig. 5 is less than 5%, except for the 900 nm ligament size sample (30 G), which was tested by Vickers indentation (to avoid indentation size effects).

### 4.3. The yield strength scaling equation

As covered in Section 4.2, nanoporous foams do not follow directly the Gibson and Ashby relationship between yield strength and relative density (Eq. (1)). In order to understand the length scale effect revealed by Fig. 5, we use Eq. (1) to calculate the yield strength of the ligaments in nanoporous Au. Fig. 6 shows a Hall–Petch-type plot of the calculated ligament yield strength ($\sigma_{yc}$) vs. the inverse square root of the ligament size ($L$). Also included in Fig. 6 is the yield strength obtained from a microcompression test on sample 30B (at about 5% compression) [20]. The calculated ligament yield strength ($\sigma_{yc}$) follows the relationship to $L^{-1/2}$, and can be expressed as

$$\sigma_{yc} = (\sigma_0 + k_{Au} \cdot L^{-1/2}) \quad (2)$$

where $\sigma_0$ is related the bulk material yield strength ($\sigma_s$), and $k_{Au}$ (MPa nm$^{1/2}$) is a material constant which describes the yield strength size-dependence in the regime of 10 nm to 1 μm.

Fitting the data shown in Fig. 6 using Eq. (2) (solid line) reveals the following Hall–Petch parameters: $\sigma_{yc}$ (MPa) = $200 + 9821L^{-1/2}$ (nm). This is consistent with previous research on nanocrystalline gold films ($k$ value of 9200 MPa nm$^{1/2}$ for 26–60 nm grains) [40] and sample-size effect studies of Au ($k$ values ranging 1900–7900 MPa nm$^{1/2}$ for 10 nm–1 μm length scales). This result indicates that the

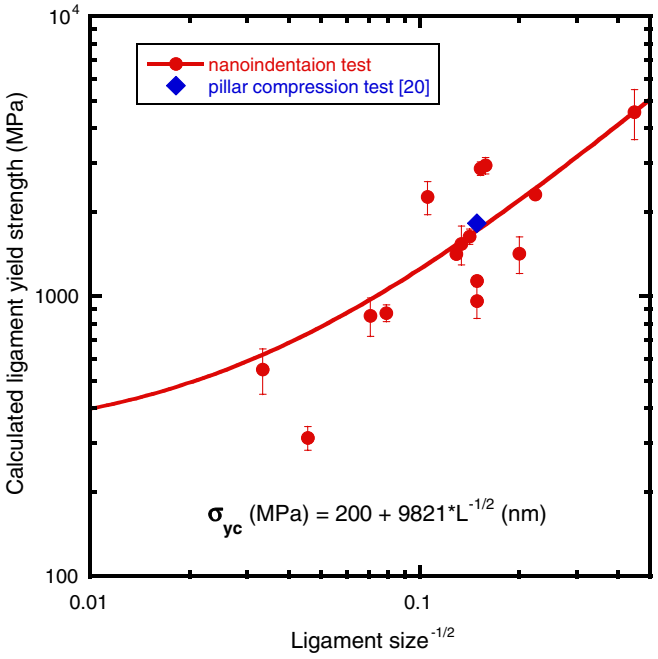


Fig. 6. Relationship of ligament size to ligament yield stress for nanoporous gold foams obtained by nanoindentation and by column microcompression testing [20].

presence of grain boundaries (nanocrystalline materials) and surfaces (sample volume effect) gives rise to very similar strengthening behavior. Combining Eqs. (1) and (2) leads to a modified foam scaling equation

$$\sigma^* = C_s[\sigma_0 + k \cdot L^{-1/2}] \cdot \left(\frac{\rho^*}{\rho_s}\right)^{3/2} \quad (3)$$

where $C_s$ is a fitting coefficient, $\sigma_0$ is the bulk material yield strength ($\sigma_s$), $k$ is the Hall–Petch-type coefficient for the theoretical yield strength of Au in the regime (10 nm to 1 μm) and $L$ is the ligament size. For macroporous foams ($L \gg 500$ nm), $k \times L^{-1/2}$ becomes negligible and Eq. (3) yields Eq. (1).

### 4.4. Foam ligaments as a high-strength material

Factors in addition to the ligament size that could give rise to the high strength of the nanoporous materials include: grain size, testing method and densification. The agreement with the microcompression tests indicates that the effect is not an indentation size effect. The fact that the increase of strength with decreasing ligament size is observed for a fixed initial foam density reveals that the defect cannot be due to densification effects. In a previous publication we have presented that our particular foam processing method produces ligaments that have a nanocrystalline grain structure [41]. The grain structure or lack thereof during dealloying is still a subject of debate and is beyond the scope of this paper [14]. However, even if we assume the ligaments are nanocrystalline, it still does not account for the high strength found experimentally since the yield strength of a nanocrystalline Au sample [41,42] is only four times higher than that of coarse-grained Au.

The increase in hardness in the nanoporous gold foam can be attributed to many factors. However, one can apply a new approach to the discussion about the increase in strength by visualizing the foam as a three-dimensional network of high-strength ligaments, as proposed by Biener et al. [20]. Recent developments from tests performed on ultrafine and micron size (180 nm to 8 μm) single crystal gold pillars prepared by FIB have demonstrated a strong pillar size dependence on the material strength. As the pillar size decreases, the yield strength of the pillar approaches the theoretical yield strength of Au [2,4]. Due to FIB size fabrication limits, the tested columns are larger than a typical foam ligament size, thus preventing a complete size comparison between both methods. However, in the overlapping length scale range (200 nm–1 μm), we observe good agreement between the calculated ligament yield strength and the single-crystal column microcompression tests [2].

The effect of the ligament size on ligament strength is evident; however, the mechanisms are not well understood. There are two general categories of explanations for such a size effect. Either (1) the dislocations are depleted from the small sample volumes and deformation is limited by dislocation source activation, as is typically observed in fine-grained materials; or (2) the dislocations interact and pile up, and high dislocation densities are required to explain the high stresses. Whether the ligament surface allows or hinders dislocation, egression will play a decisive role in the dominating deformation mechanism. Reliable TEM observations can generally distinguish between the two scenarios; however, a detailed understanding of the strengthening effect, particularly in the complex foam geometry, will require computer simulation studies. In order to unify data from nanoporous foam and single pillar compression tests, we will present MD simulations and quasi-continuum simulations in a future publication.

## 5. Conclusions

We have presented a comprehensive study of nanoporous Au foams with relative densities ranging from 20% to 42% and ligament sizes ranging from 10 to 900 nm. We observe that, at the nanoscale, the strength is controlled not only by the relative foam density (as in the case of macrocellular foams), but also by the ligament length scale. In order to account for this length scale effect, we modify the Gibson and Ashby scaling equation by incorporating a Hall–Petch-type relation ($\sigma_0 + k_{Au} \times L^{-1/2}$). In general, our results indicate that the presence of grain boundaries (nanocrystalline materials) and surfaces (sample volume effect) give rise to very similar strengthening behavior.

Testing effects were also evaluated in order to substantiate the significance of the experimental results. Nanoindentation is shown to be a valid testing technique for

low-density nanoporous materials as long as the proper parameter space is used. Overall, nanoporous Au foams are presented as a new type of high-strength, low-density material with a possibility of use in a wide range of applications.

## Acknowledgements

This work was performed under the auspices of the US Department of Energy by University of California, Lawrence Livermore National Laboratory under Contract W-7405-Eng-48. The authors thank J. Ferreira for SEM, J.A. Caro for sample characterization; and Drs. L.M. Hsiung, L. Zepeda, F. Abrahimi and Y.M. Wang at LLNL and Professor L. Gibson at MIT for helpful discussions.

## References

[1] Uchic MD et al. Science 2004;305:986.
[2] Volkert CA, Lilleodden E. Philos Mag A 2006;86:5567.
[3] Nix WD, Gao H. J Mech Phys Solids 1998;46:411.
[4] Greer JR, Oliver WC, Nix WD. Acta Mater 2005;53:1821.
[5] Manika I, Maniks J. Acta Mater 2006;54:2049.
[6] Suryanarayana C. Inter Mater Rev 1995;40:41.
[7] Kumar KS, Van Swygenhoven H, Suresh S. Acta Mater 2003;51:5743.
[8] Gibson LJ, Ashby MF. Cellular solids: structures and properties. 2nd ed. Cambridge: Cambridge University Press; 1997.
[9] Andrews EW, Gibson LJ, Ashby MF. Acta Mater 1999;47:2853.
[10] Andrews EW, Huang JS, Gibson LJ. Acta Mater 1999;47:2927.
[11] Andrews E, Sanders W, Gibson LJ. Mater Sci Eng A 1999;270:113.
[12] Zhu HX, Mills NJ. J Mech Phys Solids 1999;47:1437.
[13] Zhu HX, Hobdell JR, Windle AH. Acta Mater 2000;48:4893.
[14] Hodge AM et al. Adv Eng Mater 2006;8:853.
[15] Ding Y, Kim Y-J, Erlebacher J. Adv Mater 2004;16:1897.
[16] Li R, Sieradzki K. Phys Rev Lett 1992;68:1168.
[17] Biener J et al. J Appl Phys 2005;97:024301.
[18] Biener J, Hodge AM, Hamza AV. Appl Phys Lett 2005;87:121908.
[19] Volkert CA et al. Appl Phys Lett 2006;89:061920.
[20] Biener J et al. Nano Lett 2006;6:2379.
[21] Newman RC, Corcoran SG. MRS Bull 1999;24:24.
[22] Sieradzki K et al. J Electrochem Soc 2002;149:B370.
[23] Oliver WC, Pharr GM. J Mater Res 1992;7:1564.
[24] Savitskii EM, editor. Handbook of precious metals. New York: Hemisphere Publishing Corporation; 1989.
[25] Davies JR, editor. Metals handbook. Materials Park (OH): ASM International; 1998. p. 626.
[26] Andrews EW et al. Int J Mech Sci 2001;43:701.
[27] Liu Z, Chuah CSL, Scalon MG. Acta Mater 2003;51:365.
[28] Wilsea M, Johnson KL, Ashby MF. Int J Mech Sci 1975;17:457.
[29] Toivola Y, Stein A, Cook RF. J Mater Res 2004;19:260.
[30] Ramamurty U, Kumaran MC. Acta Mater 2004;52:181.
[31] Chen X, Xiang Y, Vlassak JJ. J Mater Res 2006;21:715.
[32] Kumar PS, Ramachandra S, Ramamurty U. Mater Sci Eng A 2003;347:330.
[33] Brydon AD et al. J Mech Phys Solids 2005;53:2638.
[34] Gioux G, McCormack TM, Gibson LG. Int J Mech Sci 2000;42:1097.
[35] Miller RE. Int J Mech Sci 2000;42:729.
[36] Erlebacher J et al. Nature 2001;410:450.
[37] Weissmueller J et al. Science 2003;300:312.
[38] Yamada Y et al. JIM 2000;41:1136.
[39] Nieh TG, Higashi K, Wadsworth J. Mater Sci Eng A 2000;283:105.
[40] Sakai Y, Tanimoto H, Mizubayashi H. Acta Mater 1999;47:211.
[41] Hodge AM et al. J Mater Res 2005;20:554.
[42] Tanimoto H et al. Mater Sci Eng A 1996;217–218:108.